Journal of Thermal Analysis and Calorimetry
https://doi.org/10.1007/s10973-024-13286-2

Exploring the response of PACAP on thermal endurance of F-actin by differential scanning calorimetry

Péter Bukovics[1] · **Dénes Lőrinczy**[1]

Received: 22 December 2023 / Accepted: 14 May 2024

Abstract
Pituitary adenylate cyclase-activating polypeptide (PACAP) is a bioactive peptide known for its diverse effects on the nervous system. While numerous studies have demonstrated the neuroprotective properties of PACAP, its role in tissue regeneration and potential as a therapeutic agent remain to be fully understood. Specifically, the understanding of PACAP's impact on cytoskeletal dynamics, particularly the organization and disorganization of actin filament networks, is limited due to the scarcity of in vitro studies in this area. Additionally, the interaction between PACAP and actin has been minimally explored, and the influence of PACAP on the thermal stability of actin is completely unknown. To address these gaps, the current study aimed to investigate the impact of different forms and fragments of PACAP on the thermal denaturation and renaturation of Ca^{2+}-F-actin using a differential scanning calorimetry (DSC) approach. Our primary objective was to determine whether PACAP modulates the thermal stability of Ca^{2+}-F-actin and establish a temperature-dependent pattern of any structural alterations that may occur as a result of PACAP interaction. Two PACAP forms exist in vivo: the 38 amino acid length PACAP38 and the PACAP27, the latter truncated at the C-terminal. Both in the PACAP38 + Ca^{2+}-F-actin and in the PACAP6-38 + Ca^{2+}-F-actin mixtures, the DSC scans exhibited a significant decrease of actin denaturation temperature compared to the control; however, the PACAP27 + Ca^{2+}-F-actin and PACAP6-27 + Ca^{2+}-F-actin revealed no remarkable differences compared to the actin control sample. The calorimetric enthalpy of the truncated PACAP27 and PACAP6-27 + actin mixture also followed the tendencies mentioned above. Thus, in PACAP27 and PACAP6-27 mixture, there was no change in the denaturation temperature of actin, and no significant ΔH_{cal} was observed. Through this research, we sought to elucidate the underlying mechanisms of PACAP's effects on actin dynamics using thermal de- and renaturation cycles.

Keywords PACAP · Filamentous actin · DSC · Cytoskeleton · Calorimetric enthalpy · Thermal unfolding

Introduction

Pituitary adenylate cyclase-activating polypeptide (PACAP) is a neuropeptide widely distributed in the nervous system, initially identified in the hypothalamus [1, 2]. Within this region, PACAP was found to activate cyclic adenosine monophosphate (cAMP) in the anterior pituitary, at the same time stimulating the release of pituitary hormones. PACAP induces cAMP levels in anterior pituitary cells, playing a determinant role in hormonal release [3]. Two biologically active forms of PACAP exist, consisting of 38 amino acids (PACAP38) and 27 amino acids (PACAP27). PACAP38 predominates and undergoes internal cleavage amidation, resulting in the formation of the PACAP27 fragment [4–7].

Belonging to the VIP/secretin/glucagon superfamily, PACAP shares structural similarities with vasoactive intestinal polypeptide (VIP) [4, 6, 8]. The antagonist form of PACAP, spanning residues 6–38, exerts potent inhibitory effects [9].

Filamentous actin (F-actin) serves as a fundamental architectural component of the cellular cytoskeleton, playing a crucial role in maintaining cellular shape, structural integrity, and dynamic cellular processes. F-actin, assembled by polymerization from globular actin (G-actin) subunits, forms long, helical filaments that contribute to the mechanical strength and stability of the cell. An intricate network of F-actin filaments extends throughout the cytoplasm,

✉ Dénes Lőrinczy
denes.lorinczy@aok.pte.hu

Péter Bukovics
peter.bukovics@aok.pte.hu

[1] Department of Biophysics, Medical School, University of Pécs, Szigeti Str. 12, Pécs H-7624, Hungary

Published online: 02 June 2024

providing a scaffold for various cellular structures and facilitating essential cellular functions [10–15].

The dynamic nature of F-actin is integral to cytoskeletal dynamics, allowing cells to adapt to changes in their environment and undergo processes such as cell migration, division, and intracellular transport. Through the coordination of polymerization and depolymerization processes, F-actin undergoes continuous remodeling, enabling cells to respond to external and internal signals [15, 16]. In addition, F-actin interacts with numerous regulatory proteins, influencing its organization, and is involved in various cellular activities, including the formation of membrane protrusions, cell adhesion, and the maintenance of cell polarity [17]. The versatile and dynamic nature of F-actin underscores its importance in orchestrating the complex ballet of cellular movements and maintaining the overall structural and functional integrity of the cell [17–20].

Effects of PACAP on F-actin dynamics. The investigation of the interaction between PACAP and F-actin represents a significant advance in understanding the complex dynamics of cellular processes. PACAP, a neuropeptide with diverse physiological functions, has been extensively studied for its effects on cell behavior and signaling pathways. The cytoskeletal system, which includes dynamic elements such as actin filaments and microtubules, plays a key role in organizing cellular functions [21–28]. To understand the effect of PACAP on F-actin, we delve into fundamental aspects of PACAP and the cytoskeletal system.

PACAP is emerging as a key regulator of neuronal processes, neurovascularization, and neurogenesis [4, 6, 8, 29]. Its role in modulating the cytoskeletal framework, particularly F-actin, offers a captivating avenue for discovery. F-actin, an essential component of the cytoskeleton, is known for its involvement in cellular motility, structural integrity, and signal transduction. Understanding the interaction between PACAP and F-actin holds promise for unraveling novel insights into cell dynamics.

Our in vitro study investigating the effect of PACAP on the thermal stability of F-actin with differential scanning calorimetry (DSC) provides a solid basis for the continuation of our exploration. Previous research has demonstrated the effect of PACAP on the reorganization of the actin filament network, with potential implications for cell migration events [21, 22, 25, 28]. The examination of neuritogenesis, neurovascularization, and neurogenesis in response to PACAP sheds light on the broader physiological consequences of this interaction [28, 30].

The central element of our study is the analysis of the expression pattern of PACAP-induced cytoskeletal elements. This includes the thermodynamics of F-actin, following polymerization. By elucidating these mechanisms, we will comprehensively understand the multiple effects of PACAP on cytoskeletal architecture as well as its downstream effects on cell behavior.

In this manuscript, we set out to explore the nuanced relationships between PACAP and F-actin using a methodology similar to previous studies focusing on actin monomers. The convergence of PACAP-driven changes in actin dynamics with broader cellular phenomena such as neuritogenesis and neurovascularization creates a compelling narrative of the effects of PACAP on cellular function. By exploring these complexities in detail, we aim to contribute to the evolving landscape of knowledge in the field of biophysics and cell biology.

Materials and methods

The extraction of Ca^{2+}-G-actin from rabbit striated muscle followed a meticulously established protocol in our laboratory [31–33]. The MOPS buffer, a crucial component for actin extraction and stabilization, was formulated with MOPS (3-(N-morpholino) propane sulfonic acid) as the buffering agent, $CaCl_2$ for maintaining physiologically relevant calcium ion concentrations, MEA (β-mercaptoethanol) as a reducing agent, and NaN_3 to prevent bacterial contamination. ATP (adenosine triphosphate) was also included in the buffer to sustain actin in its active state. The actin preparation encompassed the addition of 50 mM KCl and 2 mM $MgCl_2$ to ensure optimal actin stability throughout the experiments. Rigorous measures were implemented to ascertain the purity and integrity of the Ca^{2+}-G-actin sample, ensuring the robustness and precision of subsequent examinations into the impact of PACAP on F-actin thermodynamics.

The pH of the buffer was meticulously set at 7.8, a critical parameter for establishing a biologically relevant and controlled environment conducive to studying actin dynamics and its interactions with PACAP. Before the experiment, overnight G-actin polymerization was induced by solutions of KCl and $MgCl_2$ at final concentrations of 100 mM and 2 mM, respectively. This pre-experimental step ensured the stability of F-actin, enhancing the reliability of results.

PACAP information, including the applied forms and fragments along with their respective amino acid sequences, can be referenced in Fig. 1.

Differential scanning calorimetry (DSC) measurements were conducted using the SETARAM Micro DSC-III in a temperature range of 0–110 °C, employing a scanning rate of 0.3 $Kmin^{-1}$ over two heating/cooling cycles. Denaturation experiments were carried out in conventional Hastelloy batch vessels, with an average sample volume of 950 µL. The MOPS buffer served as the reference sample, and both the sample and reference were equilibrated with

1	10 20	30	
HSDGI	FTDSYSRYRKQMAVKKYLAAVL	GKRYKQRVKNK	PACAP 1-38
HSDGI	FTDSYSRYRKQMAVKKYLAAVL		PACAP 1-27
	FTDSYSRYRKQMAVKKYLAAVL		PACAP 6-27
	FTDSYSRYRKQMAVKKYLAAVL	GKRYKQRVKNK	PACAP 6-38

Fig. 1 The amino acid sequences of various PACAP isoforms: PACAP 1–38 (P38, the bioactive full-length natural isoform), PACAP 1–27 (P27, a natural bioactive fragment), PACAP 6–27 (P6-27, an artificial fragment), and PACAP 6–38 (P6-38, an artificial fragment)

a precision of ± 0.1 mg. A buffer–buffer set was utilized as a baseline reference, subtracted from the original DSC curve. The heat flow, recorded as a function of temperature using the hermetically closed vessels of the DSC-III heat flux instrument, was plotted. Calorimetric enthalpy was calculated by integrating the area under the heat flow curve using a two-point setting with SETARAM peak integration. All presented results are expressed as mean values ± standard error (s.d.), with three measurements conducted for each case.

To evaluate thermal stability and interactions, Ca^{2+}-F-actin was consistently maintained at a concentration of 2 mg mL^{-1} at pH 7.8 across all experiments. This concentration ensured methodological consistency in DSC analyses, enabling meaningful comparisons throughout the experimental framework. The PACAP peptide was applied at a concentration of 21 µM at pH 7.8, strategically chosen to explore potential interactions with actin under controlled conditions. Employing a highly sensitive calorimeter, DSC measurements were conducted to precisely assess the thermal denaturation and renaturation of Ca^{2+}-F-actin in the presence of PACAP. The adoption of standardized concentrations facilitated robust and reproducible data acquisition, contributing to a comprehensive understanding of how PACAP influences actin stability and potential regulatory mechanisms within the cytoskeleton.

Results

The thermal phenomena accompanying the interaction of F-actin and PACAP took place in the range of 40–80 °C. Neither the first cooling nor the repeated second heating–cooling cycle showed any signs of thermal structural change, so only this range was taken into account in the evaluation (because the first cooling exhibited an irreversible denaturation). Figure 2 and Table 1 present a consolidated overview of the denaturation measurements for physiologically significant PACAP compounds across heating–cooling cycles. Given the baseline reproducibility of our DSC at approximately 2–3 µW, additional tests are warranted to validate values within this proximity, providing further support for the selection of the 40–80 °C temperature range (this is another argument in favor of choosing the 40–80 °C range).

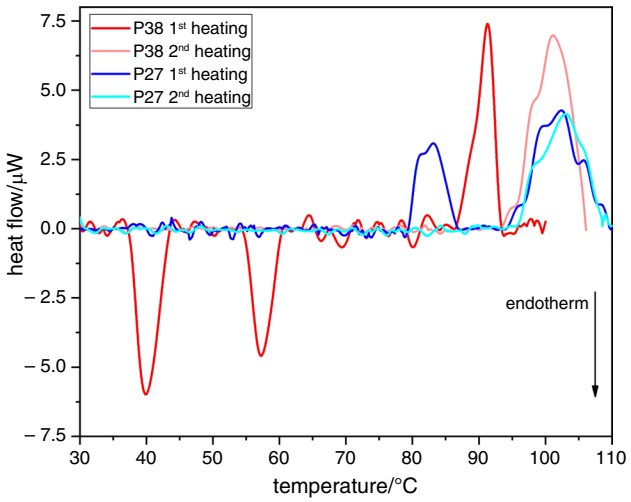

Fig. 2 Denaturation curves for PACAP38 and PACAP27 fragments, with the curves representing averages in the first and second heating cycles. (c_{PACAP} = 21 µM; c_{actin} = 2 mg mL^{-1}; pH = 7.8; V_{sample} = 950 µL)

PACAP38 displayed two endothermic peaks during the initial heating, observed at around 40 and 57 °C, along with an exothermic peak at 91 °C. The lower endotherm could be assigned to the denaturation of 1–27 (N-terminal part) unit, while the higher one to the 28–38 (C-terminal part). The big difference between the two peaks is the sign of weak cooperativity between them (the first denaturation has not any influence on the second thermodynamic domain of PACAP38). The exotherm peak can demonstrate the rearrangement of N-terminal into more compact structure. Surprisingly, no detectable effect was noted during the first cooling; however, in the second heating cycle, the lower-temperature denaturation events were eliminated, indicating irreversible changes post the initial heating, and the exothermic peak shifted to a higher temperature (approximately 101 °C). In contrast, PACAP27 exhibited no endothermic peaks but displayed

Table 1 The thermal characteristics of various PACAP variants at a concentration of 21 µM

Samples	Thermal parameters							
	T_{mL1}/°C	ΔH_{L1}/Jg^{-1}	T_{mL2}/°C	ΔH_{L2}/Jg^{-1}	T_{mH1}/°C	ΔH_{H1}/Jg^{-1}	T_{mH2}/°C	ΔH_{H2}/Jg^{-1}
PACAP38 1st h	40.1 ± 0.3	0.008 ± 0.001	56.7 ± 0.4	0.006 ± 0.001	90.8 ± 0.5	− 0.012 ± 0.001	–	–
PACAP38 2nd h	–	–	–	–	–	–	101.1 ± 0.7	− 0.023 ± 0.002
PACAP27 1st h	–	–	–	–	83.7 ± 0.4	− 0.005 ± 0.001	102.9 ± 0.6	− 0.007 ± 0.001
PACAP27 2nd h	–	–	–	–	–	–	103.1 ± 0.7	− 0.006 ± 0.001

Notations include h/c for heating/cooling cycle, T_m denotes the melting (denaturation peak) temperature, and L and H indicate lower and higher temperature ranges, respectively. ΔH represents calorimetric enthalpy, and all values are averages from three measurements ± standard deviation. Negative signs denote exothermic transitions

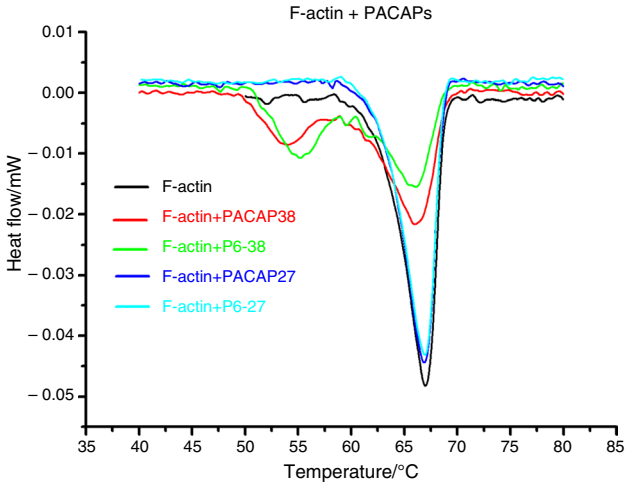

Fig. 3 The denaturation curves of Ca^{2+}-F-actin and its complexes with different PACAP fragments during the first heating cycles. (c_{PACAP} = 21 µM; c_{actin} = 2 mg mL^{-1}; pH = 7.8; V_{sample} = 950 µL)

Table 2 Thermal parameters of 2 mg mL^{-1} (46 µM) Ca^{2+}-F-actin (green) and its mixing with different PACAP of 21 µM

Samples	Thermal parameters		
	T_{mL}/°C	T_{mH}/°C	Total ΔH/Jg^{-1}
Ca^{2+}-F-actin	–	**67.0 ± 0.2**	**0.0393 ± 0.003**
F-actin-PACAP38 1st h	54.1 ± 0.3	**66.2 ± 0.3**	0.0383 ± 0.006
F-actin-PACAP6-38 1st h	**55.1 ± 0.4**	**66.1 ± 0.3**	0.0321 ± 0.005
F-actin-PACAP27 1st h	–	66.9 ± 0.3	0.0375 ± 0.004
F-actin-PACAP6-27 1st h	–	67.0 ± 0.3	0.0371 ± 0.003

Symbols: h-heating cycle, *L* and *H* stand for lower and higher temperature range, T_m is melting (denaturation) temperature as well, and ΔH is the total calorimetric enthalpy normalized on sample mass. Data are averages of three measurements ± s.d

two exothermic peaks during the first heating. In the second heating cycle, the first exothermic peak disappeared, while the second persisted at the same temperature with nearly identical ΔH_{cal}. All observed effects fell within the range of instrument error. These findings suggest that these two derivatives possess a highly stable core from a thermal standpoint, a characteristic supported by their interaction with F-actin (refer to Fig. 3 and Table 2) and referring to the high-temperature exothermic transitions which might originate from self-aggregated peptides.

In Fig. 3, the summarized result of the denaturation measurements can be seen performed on Ca^{2+}-F-actin mixed with PACAP compounds having physiologically relevant concentration. The Ca^{2+}-F-actin exhibited only a usual denaturation peak (T_m) around 67 °C with 0.0393 Jg^{-1} calorimetric enthalpy (ΔH_{cal}) [34–37].

The denaturation of Ca^{2+}-F-actin alone was irreversible, we did not detect a thermal signal neither during the first cooling nor during the second heating and cooling cycle. In addition to the control Ca^{2+}-F-actin alone, Ca^{2+}-F-actin + PACAP38 mixture exhibited double endotherm peaks: a lower at 54.1 and a higher at 66.2 °C (see Fig. 3 and Table 2.). The lower one is a typical G-actin denaturation temperature [34], indicating the presence of partly depolymerized actin, while the higher peak reports the weakening of the structure of F-actin because of the binding of PACAP into the nucleotide-binding pocket of actin protomer (the original denaturation temperature decreased ~ by 1 °C).

The whole denaturation temperature range decreased by ~ 7 °C, which also supports the view that addition of PACAP38, the actin structure becomes less compact. The calorimetric enthalpy exhibited a remarkable decrease in the case of PACAP6-38, compared to F-actin. The first T_m became higher, but the second one remained the same (indicating the strong effect of PACAP38 in the loosening of the internal structure of actin monomers (see Table 2. and Fig. 3).

We did not observe the strong thermal effect on Ca^{2+}-F-actin by the other PACAP27 forms, which may emphasize the higher physiological importance of PACAP38. The PACAP27 fragments produced only one endotherm. The endotherm's T_m was a bit higher than in the case of PACAP38 with a closely same ΔH_{cal} (see Fig. 3. and Table 2), but no significant difference compared with

F-actin. It means that its structural effect on F-actin is negligible.

The first DSC scans of PACAP6-27 produced also the same basic effect as was observed at F-actin: T_m and ΔH_{cal} are in the F-actin range (see Fig. 3 and Table 2).

Discussion

In this research, we systematically explored the impact of different PACAP fragments on the thermal stability of Ca^{2+}-F-actin through differential scanning calorimetry. Additionally, we examined the standalone thermal stability of these various PACAP forms and fragments, independent of Ca^{2+}-F-actin.

The DSC experiments conducted on physiologically relevant PACAP compounds in the absence of actin unveiled intriguing thermal profiles. These outcomes suggest that both PACAP38 and PACAP27 possess transition into an exceptionally stable core, likely attributed to the N-terminal segments (amino acids 1–27) of their structure (refer to Fig. 1), which are implicated in the observed exothermic process. The absence of amino acids 1–5 segment (Fig. 1) corresponds to the lack of an endothermic transition. This thermal stability is underscored by their resistance to denaturation and their interactions with F-actin. The presence of multiple thermal transitions hints at intricate structural changes or conformational rearrangements within these PACAP molecules. Further exploration is essential to unveil the precise nature and functional implications of these thermal transitions and their potential involvement in biological processes. Notably, the PACAP molecules alone exhibited subtle thermal effects within the investigated temperature range.

Concerning PACAP-Ca^{2+}-F-actin interactions, our findings revealed that Ca^{2+}-F-actin itself displayed a characteristic denaturation peak, and this denaturation was irreversible, indicating a substantial structural transformation during this process. The introduction of the active form of PACAP (PACAP38) to Ca^{2+}-F-actin led to a double endotherm peak during the first heating, possibly signifying a relaxation of the filamentous actin structure due to PACAP binding into the actin cleft. In the case of PACAP38 and PACAP6-38, this could be the consequence of PACAP binding to the cleft of actin monomer (see Fig. 4.) which can disturb the structure of the hinge between subdomains 1 and 3 and cause a loosening of the two big domains (I: subdomain 1 and 2 and II: subdomain 3 and 4) [38, 39]. The lack of exothermic effect (refer to Table 2) likely corresponds to the absence of non-bound PACAP molecules. In the second heating–cooling cycle, no effect was discerned. The effects observed during the first cooling and second heating–cooling cycles fell within the instrument error range, leading us to disregard them.

In the first heating cycle, the PACAP6-38 fragment displayed two endotherm peaks similarly to PACAP38-Ca^{2+}-F-actin having similar T_m values, despite the first one was at a slightly higher T_m (1 °C). This disparity suggests more intricate structural changes and enhanced ordering within the complex, highlighting the distinctive thermodynamic behavior of PACAP38. For the PACAP38-actin and PACAP6-38-actin interaction, this might imply more elaborate or extensive conformational changes during heating compared to the PACAP27-actin complex. Such

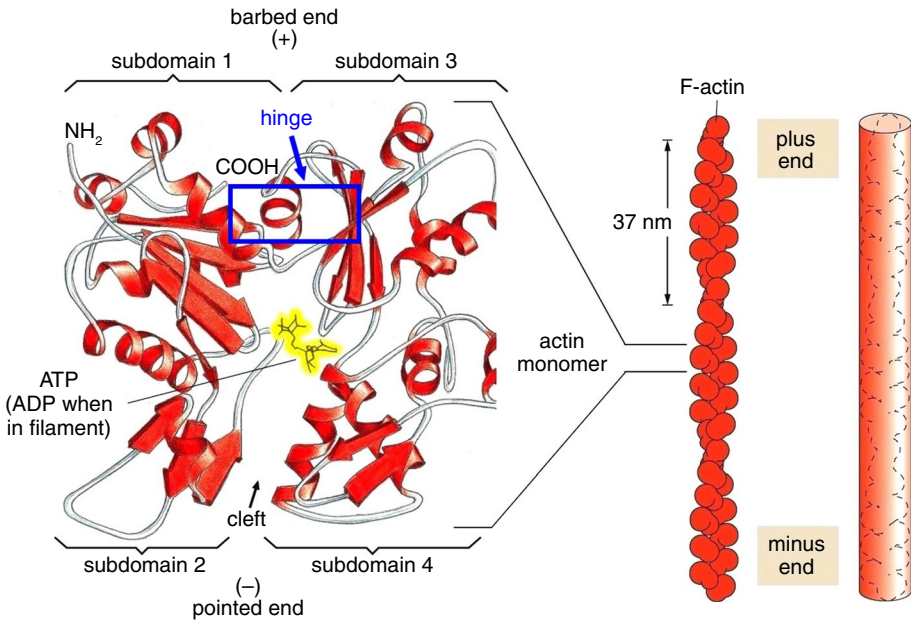

Fig. 4 The structure of G- and F-actin. (The modified image is based on the following sources: https://neherlab.org/20171031_theoretical_biophysics.html; https://hu.m.wikipedia.org/wiki/F%C3%A1jl:G-actin_subdomains.png)

changes could involve the initiation of a larger number of bonds or interactions among PACAP molecules. Our findings demonstrate that the PACAP27 and PACAP6-27 fragments, despite showcasing a denaturation temperature (T_m) akin to that of Ca^{2+}-F-actin alone, exhibited similar calorimetric enthalpy. These thermodynamic differences imply reduced energy demands for structural transformations during denaturation in case of PACAP38 and 6–38. Notably, the absence of any exothermic signal and the similarities to Ca^{2+}-F-actin denaturation pattern indicate the lack of any structural effect of PACAP27 and PACAP6-27 on F-actin.

Consistent with earlier in vitro investigations [21–28], our study affirms the significant impact of PACAP38 and PACAP6-38 on the thermal stability of actin filaments, inducing notable changes in both structural features and denaturation behavior. These alterations have the potential to elicit functionally significant conformational changes in actin. However, a thorough examination of these effects calls for further comprehensive research.

Conclusions

In this paper, we systematically investigated the influence of different PACAP fragments on the thermal stability of Ca^{2+}-F-actin using differential scanning calorimetry. Additionally, we examined the standalone thermal stability of various PACAP forms and fragments, independent of Ca^{2+}-F-actin which revealed intriguing thermal profiles, indicating that both PACAP38 and PACAP27 possess a remarkably stable core likely attributed to their N-terminal segments (amino acids 1–27). This stability, evidenced by resistance to denaturation and interactions with F-actin, hints at intricate structural changes within these PACAP molecules, requiring further exploration. Notably, PACAP molecules alone exhibited subtle thermal effects within the investigated temperature range.

Our study is the first to explore actin-PACAP interactions using a thermoanalytical method. Findings reveal intricate interplay between PACAP forms and/or fragments and actin, influencing actin's thermal stability. This shift is crucial in understanding how PACAP variants influence actin filaments. PACAP38 and PACAP6-38 demonstrated the most pronounced effects on actin thermal stability. Other PACAP forms and fragments (PACAP27 and PACAP6-27) had no significant impact on Ca^{2+}-F-actin. These insights into diverse interactions between PACAP and actin provide valuable thermodynamic dynamics understanding.

In summary, our results indicate that the interaction between PACAP and actin goes beyond a simple additive effect of their individual properties, involving specific interactions that alter the overall stability of the system. Further research is imperative to meticulously characterize these interactions and understand their functional consequences, necessitating additional experiments.

Acknowledgements The authors are grateful to Andrea Tamás for providing PACAP. This work was supported by CO-272 (OTKA) grant (DL).

Authors' contributions **PB**, rising the problem, contributed to the sample preparation and handling, data analysis, and manuscript writing. **DL**, corresponding author and principal investigator, contributed to the DSC experiments, data analysis, and manuscript writing

Funding Open access funding provided by University of Pécs.

Data availability There are no additional available data to upload.

Declarations

Conflict of interest The authors declare that they have no known competing financial interests or personal relationships that could have appeared to influence the work reported in this paper.

Consent for publication The copyright form has been uploaded with the manuscript.

References

1. Miyata A, Jiang L, Dahl RD, Kitada C, Kubo K, Fujino M, et al. Isolation of a neuropeptide corresponding to the N-terminal 27 residues of the pituitary adenylate cyclase activating polypeptide with 38 residues (PACAP38). Biochem Biophys Res Commun. 1990;170:643–8.
2. Ohkubo S, Chiharukimura K, Ogi K, Okazaki K, Masakihosoya F, Onda H, et al. Primary structure and characterization of the precursor to human pituitary adenylate cyclase activating polypeptide. DNA Cell Biol. 1992;11:21–30.
3. Miyata A, Arimura A, Dahl RR, Minamino N, Uehara A, Jiang L, et al. Isolation of a novel 38 residue-hypothalamic polypeptide which stimulates adenylate cyclase in pituitary cells. Biochem Biophys Res Commun. 1989;164:567–74.
4. Wang J, Song X, Zhang D, Chen X, Li X, Sun Y, et al. Cryo-EM structures of PAC1 receptor reveal ligand binding mechanism. Cell Res. 2020;30:436–45.
5. Hamelink C, Lee H-W, Chen Y, Grimaldi M, Eiden LE. Coincident elevation of cAMP and calcium influx by PACAP-27 synergistically regulates vasoactive intestinal polypeptide gene transcription through a novel PKA-independent signaling pathway. J Neurosci. 2002;22:5310–20.

6. Handbook of Biologically Active Peptides [Internet]. [cited 2022 Dec 28]. Available from: https://www.nhbs.com/handbook-of-biologically-active-peptides-book-2
7. Arimura A. Pituitary adenylate cyclase activating polypeptide (PACAP): discovery and current status of research. Regul Pept. 1992;37:285–303.
8. Vaudry D, Falluel-Morel A, Bourgault S, Basille M, Burel D, Wurtz O, et al. Pituitary adenylate cyclase-activating polypeptide and its receptors: 20 years after the discovery. Pharmacol Rev. 2009;61:283–357.
9. Sun C, Song D, Davis-Taber RA, Barrett LW, Scott VE, Richardson PL, et al. Solution structure and mutational analysis of pituitary adenylate cyclase-activating polypeptide binding to the extracellular domain of PAC1-RS. Proc Natl Acad Sci. 2007;104:7875–80.
10. Stricker J, Falzone T, Gardel ML. Mechanics of the F-actin cytoskeleton. J Biomech. 2010;43:9–14.
11. THE STRUCTURE OF F-ACTIN - ProQuest [Internet]. [cited 2023 Nov 10]. Available from: https://www.proquest.com/openview/2cf5572f1584cf28668c15ca8f84af11/1?cbl=18750&diss=y&pq-origsite=gscholar&parentSessionId=FGbQVYuoDnSoddQFM2OGWoDU62Ufp3Fv537ksmtSgw%3D
12 Hanson J, Lowy J. The structure of F-actin and of actin filaments isolated from muscle. J Mol Biol. 1963;6:46-IN5.
13. Riedl J, Crevenna AH, Kessenbrock K, Yu JH, Neukirchen D, Bista M, et al. Lifeact: a versatile marker to visualize F-actin. Nat Methods. 2008;5:605–7.
14. Galkin VE, Orlova A, Schröder GF, Egelman EH. Structural polymorphism in F-actin. Nat Struct Mol Biol. 2010;17:1318–23.
15. Hayden SM, Miller PS, Brauweiler A, Bamburg JR. Analysis of the interactions of actin depolymerizing factor with G- and F-actin. Biochemistry. 1993;32:9994–10004.
16. Robaszkiewicz K, Ostrowska Z, Marchlewicz K, Moraczewska J. Tropomyosin isoforms differentially modulate the regulation of actin filament polymerization and depolymerization by cofilins. FEBS J. 2016;283:723–37.
17. Bezanilla M, Gladfelter AS, Kovar DR, Lee W-L. Cytoskeletal dynamics: a view from the membrane. J Cell Biol. 2015;209:329–37.
18. Civelekoglu G, Edelstein-Keshet L. Modelling the dynamics of F-actin in the cell. Bltn Mathcal Biology. 1994;56:587–616.
19. Maruthamuthu V, Aratyn-Schaus Y, Gardel ML. Conserved F-actin dynamics and force transmission at cell adhesions. Curr Opin Cell Biol. 2010;22:583–8.
20. Lemieux MG, Janzen D, Hwang R, Roldan J, Jarchum I, Knecht DA. Visualization of the actin cytoskeleton: different F-actin-binding probes tell different stories. Cytoskeleton. 2014;71:157–69.
21. Falluel-Morel A, Vaudry D, Aubert N, Galas L, Benard M, Basille M, et al. PACAP and ceramides exert opposite effects on migration, neurite outgrowth, and cytoskeleton remodeling. Ann N Y Acad Sci. 2006;1070:265–70.
22. Perez V, Bouschet T, Fernandez C, Bockaert J, Journot L. Dynamic reorganization of the astrocyte actin cytoskeleton elicited by cAMP and PACAP: a role for phosphatidylInositol 3-kinase inhibition. Eur J Neurosci. 2005;21:26–32.
23. Sakai Y, Hashimoto H, Shintani N, Katoh H, Negishi M, Kawaguchi C, et al. PACAP activates Rac1 and synergizes with NGF to activate ERK1/2, thereby inducing neurite outgrowth in PC12 cells. Brain Res Mol Brain Res. 2004;123:18–26.
24. Li H-X, Feng J, Liu Q, Ou B-Q, Lu S-Y, Ma Y. PACAP-derived mutant peptide MPAPO protects trigeminal ganglion cell and the retina from hypoxic injury through anti-oxidative stress, anti-apoptosis, and promoting axon regeneration. Biochim Biophys Acta Gen Subj. 2021;1865: 130018.
25. Falluel-Morel A, Vaudry D, Aubert N, Galas L, Benard M, Basille M, et al. Pituitary adenylate cyclase-activating polypeptide prevents the effects of ceramides on migration, neurite outgrowth, and cytoskeleton remodeling. Proc Natl Acad Sci. 2005;102:2637–42.
26. Fabian E, Reglodi D, Horvath G, Opper B, Toth G, Fazakas C, et al. Pituitary adenylate cyclase activating polypeptide acts against neovascularization in retinal pigment epithelial cells. Ann N Y Acad Sci. 2019;1455:160–72.
27. Héraud C, Hilairet S, Muller J-M, Leterrier J-F, Chadéneau C. Neuritogenesis induced by vasoactive intestinal peptide, pituitary adenylate cyclase-activating polypeptide, and peptide histidine methionine in SH-SY5y cells is associated with regulated expression of cytoskeleton mRNAs and proteins. J Neurosci Res. 2004;75:320–9.
28. Toriyama M, Mizuno N, Fukami T, Iguchi T, Toriyama M, Tago K, et al. Phosphorylation of doublecortin by protein kinase A orchestrates microtubule and actin dynamics to promote neuronal progenitor cell migration. J Biol Chem. 2012;287:12691–702.
29. Vaudry D, Gonzalez BJ, Basille M, Yon L, Fournier A, Vaudry H. Pituitary adenylate cyclase-activating polypeptide and its receptors: from structure to functions. Pharmacol Rev. 2000;52:269–324.
30. Braas KM, May V, Harakall SA, Hardwick JC, Parsons RL. Pituitary adenylate cyclase-activating polypeptide expression and modulation of neuronal excitability in guinea pig cardiac ganglia. J Neurosci. 1998;18:9766–79.
31. Spudich JA, Watt S. The regulation of rabbit skeletal muscle contraction. I. Biochemical studies of the interaction of the tropomyosin-troponin complex with actin and the proteolytic fragments of myosin. J Biol Chem. 1971;246:4866–71.
32. Vig AT, Földi I, Szikora S, Migh E, Gombos R, Tóth MÁ, et al. The activities of the C-terminal regions of the formin protein disheveled-associated activator of morphogenesis (DAAM) in actin dynamics. J Biol Chem. 2017;292:13566–83.
33. Tóth MÁ, Majoros AK, Vig AT, Migh E, Nyitrai M, Mihály J, et al. Biochemical activities of the wiskott-aldrich syndrome homology region 2 domains of sarcomere length short (SALS) protein. J Biol Chem. 2016;291:667–80.
34. Lörinczy D, Belágyi J. Scanning calorimetric and EPR studies on the thermal stability of actin. Thermochim Acta. 1995;259:153–64.
35. Lőrinczy D, Vértes Z, Könczöl F, Belágyi J. Thermal transitions of actin. J Therm Anal Calorim. 2009;95:713–9.
36. Könczöl F, Lőrinczy D, Vértes ZS, Hegyi G, Belagyi J. Intermonomer cross-linking affects the thermal transitions in F-actin. J Therm Anal Calorim. 2010;101:549–53.
37 Türmer K, Könczöl F, Lőrinczy D, Belágyi J. AMP.PNP affects the dynamical properties of monomer and polymerized actin. J Therm Anal Calorim. 2012;108:95–100.
38. Lőrinczy D, Könczöl F, Gaszner B, Belagyi J. Structural stability of actin filaments as studied by DSC and EPR. Thermochim Acta. 1998;322:95–100.
39. Lőrinczy D. Cyclophosphamide treatment evoked side effects on skeletal muscle monitored by DSC. J Thermal Anal Calorim. 2020;142:1897–901.